Systematic Diagnosis of Prostate Cancer Using an Optical Biopsy Needle Adjunct with Fluorescence Spectroscopy

Priya N. Werahera, *Senior Member IEEE*, Edward A. Jasion, E. David Crawford, Francisco G. La Rosa, M. Scott Lucia, Adrie van Bokhoven, Holly T. Sullivan, J. David Port, Paul D. Maroni, and John W. Daily

Abstract— **Transrectal ultrasound guided prostate biopsies often fail to diagnose prostate cancer with 90% of cores reported as benign. Thus, it is desirable to target prostate cancer lesions while reducing the sampling of benign tissue. The concentrations of natural fluorophores in prostate tissue fluctuate with disease states. Hence, fluorescence spectroscopy could be used to quantify these fluctuations to identify prostate cancer. An optical biopsy needle with a light sensitive optical probe at the tip of the inner needle was developed to take prostate biopsies after measuring tissue fluorescence with a laboratory fluorometer. The optical probe consists of eight 100 µm fibers for tissue excitation and a single 200 µm fiber to capture fluorescence spectra. Random biopsy cores were taken from 20 surgically excised prostates after measuring fluorescence spectra of tissue between 295-550nm for several excitations between 280-350nm. Each biopsy core was histopathologically classified and correlated with corresponding spectra. Prostate biopsies were grouped into benign or malignant based on the histological findings. Out of 187 biopsy cores, 109 were benign and 78 were malignant. Partial least square analysis of tissue spectra was performed to identify diagnostically significant principal components as potential classifiers. A linear support vector machine and leave-one-out cross validation method was employed for tissue classification. Study results show 86% sensitivity, 87% specificity, 90% negative predictive value, and 83% positive predictive value for benign versus malignant prostate tissue classification. This study demonstrates potential clinical applications of fluorescence spectroscopy guided optical biopsy needle for prostate cancer diagnosis with the consequent improvement of patient care.**

I. Introduction

Prostate cancer is the most common noncutaneous human malignancy, and the second most lethal tumor among American men [1]. In 2014, an estimated 233,000 men will be diagnosed with prostate cancer and 29,480 will die from this disease [1]. Prostate cancer is currently diagnosed by pathological examination of biopsy tissue obtained from patients suspected of having the disease. Prostate biopsies are recommended for men with a serum prostate-specific antigen (PSA) level above 4 ng/mL or with an abnormal digital rectal exam (DRE) [2]. Prostate biopsies are obtained using an 18G biopsy needle under the guidance of transrectal ultrasound (TRUS).

The standard of care requires urologists to take 10-12 TRUS biopsies per patient. The clinical prostate cancer detection rate is only 25-35%. More than 50% of cancers that need definitive therapy remain undetected during initial biopsies [3]. Such undiagnosed cancers are at high risk of spreading beyond the prostate gland and metastasizing to distant sites. Currently, there are no curative treatments available for metastatic prostate cancer [4]. Therefore, patient survival depends largely on early and accurate diagnosis of this disease.

TRUS images show only the anatomical landmarks of the prostate gland, but not the individual cancer lesions. Hence, TRUS biopsies are subject to serious sampling errors and often miss significant cancers [3]. Therefore, the main limitation of TRUS biopsies is that they are taken randomly without any prior knowledge of whether the underlying tissue is cancerous or not.

Optical spectroscopy methods can be used to determine whether underlying tissue is cancerous or not [5]. The light-tissue interaction is characterized by the physical nature of light and specific tissue morphology and composition [6]. In fluorescence spectroscopy, one or more narrowband light sources are used to excite endogenous fluorophores and the emission spectrum at each excitation wavelength is detected. The fluorescence spectra (FS) depend on several important endogenous fluorophores such as tryptophan, collagen, nicotinamide adenine dinucletide (NADH), flavin adenine dinucleotide (FAD), and others. Quantitative analysis of FS obtained from tissue can provide valuable information regarding biochemical changes that correlate with disease status [7].

Zhu *et al* used a fiber optic probe to measure FS at seven excitation wavelengths from 300 to 420 nm in 20 nm increments of breast tissues *in vivo* during percutaneous image-guided breast biopsy [8]. They analyzed a total of 121 biopsy samples with histopathology data and accompanying FS. Partial least square and support vector

Research supported by a proof-of-concept grant from the Precision Biopsy, *LLC*, a subsidiary of Allied Minds, Inc., Boston, MA.

P. N. Werahera is with the Pathology and Bioengineering Departments, University of Colorado Anschutz Medical Campus, Mail Stop 8104, P. O. Box 6511, Aurora, CO 80045. (phone: 303-724-3784; fax: 303-724-3712; e-mail: Priya.Werahera@ucdenver.edu)

E. A. Jasion is with the Precision Biopsy *LLC*, 12635 E. Montview Blvd, Aurora, CO 80045.

F. G. La Rosa, M. S. Lucia, A. van Bokhoven, and H. T. Sullivan are with the Pathology Department, P. D. Maroni is with the Division of Urology, Surgery Department, J. D. Port is with Pharmacology Department, and E. D. Crawford is with the Urologic Oncology Department, University of Colorado Anschutz Medical Campus, Aurora, CO 80045.

J. W. Daily is with the Mechanical Engineering Department, University of Colorado, Boulder, CO 80309. (e-mail: John.Daily@colorado.edu).

P. N. Werahera, M. S. Lucia, and J. W. Daily are the co-founders of Precision Biopsy *LLC*, 12635 E. Montview Blvd, Aurora, CO 80045.

978-1-4244-7929-0/14/$26.00 ©2014 IEEE

machines with leave-one-out cross validation provided sensitivity and specificity of up to 81% and 87%, respectively, for malignant versus fibrous/benign tissue classification [8]. Jayanthi *et al* used a fiber optic probe for classification of oral lesions *in vivo* employing FS for 404 nm excitation [9]. Linear discriminant analysis based on the leave-one-out method of cross validation was able to differentiate pre-malignant dysplasia from squamous cell carcinoma, benign hyperplasia from dysplasia and hyperplasia from normal with overall sensitivities of 86%, 78%, and 92%, and specificities of 90%, 100%, and 100%, respectively.

We have prototyped a 15G optical biopsy needle (an integrated optical sensor and a biopsy needle) based on FS to obtain prostate biopsies *after* the optical characterization of underlying tissue [10]. This needle was tested using surgically excised radical prostatectomy specimens. In Section II we present design and testing methods for the optical biopsy needle and spectral data analysis for prostate tissue classification. In Section III, experimental results are provided including sensitivity and specificity for prostate cancer diagnosis. Conclusions are presented in Section IV.

II. METHODOLOGY

A. Experimental Setup

Our optical biopsy needle shown in *Figure 1* consists of a 15G outer needle, slightly smaller inner needle, and two optical connectors. The inner needle has an optical sensor at the tip and a sample notch to hold the biopsy tissue. Two sets of fiber optics cables are used for excitation and capture of emission spectra of tissue. The frontend of fibers are terminated at the tip of the inner needle and arranged as the optical sensor for optical characterization of tissue. The backend of fibers are terminated with standard SMA connectors. Both inner and outer needle were tested for structural integrity and reliability. This needle interface with the BARD Urological MAGNUM® gun and can cut 22 mm long tissue cores following optical characterization of tissue.

Figure 1: Optical biopsy needle with BARD Urological MAGNUM biopsy gun

The inner needle of a standard prostate biopsy needle has been redesigned to lay fiber optic cables underneath the specimen notch. The optical sensor consists of eight 100 µm source fibers with numerical aperture (NA) of 0.22 arranged in a circle with a single 200 µm center fiber with NA of 0.22 to read the fluorescence signal. The tip of the needle is cut and polished at a 60 degree angle to facilitate tissue cutting and minimize reflective losses for light travelling from the fiber optic probe into the tissue. This critical angle was determined according to the Snell's law of refraction using refractive indices of 1.491, 1.478, and 1.385 for fiber at 290 nm, 340 nm, and mammalian HeLa cells, respectively.

Patients scheduled for radical prostatectomy surgery at the University of Colorado Hospital between April 2009 and June 2010 were consented for this study. Surgically excised prostatectomy specimens from consented patients were delivered to the lab within minutes. Optical data and corresponding tissue biopsy cores were taken within 90 min after surgical excision of the specimen.

Using a standard laboratory fluorometer (Fluorolog-3, JY HORIBA) with an optical platform, we collected FS from different anatomical locations of the prostate with corresponding tissue biopsy cores. The Fluorolog-3 contains a 450W xenon arc lamp as the excitation source, a monochromator as the excitation wavelength selector, a 2nd monochromator to select the emitted fluorescence from the sample, and an R928P photon multiplier tube in photon-counting mode as the emission detector. Background measurements were taken by inserting the biopsy needle in a test tube with deionized water. FS spectra were obtained at 280, 290, 300, 330, 340, and 350 nm excitations. Emission spectra were collected starting 15 nm higher from each excitation wavelength at 5 nm intervals up to 550 nm. We obtained spectral data and corresponding tissue biopsy cores from 10-12 different locations within each prostate specimen. The distal-end of each biopsy core was inked and put inside a specimen vial containing 10% neutral buffered formalin (NBF). Each specimen vial was labeled accordingly to correlate with spectral data. After data collection, the prostate specimen was placed in a specimen container with 10% NBF.

For histopathological classification, standard hematoxylin and eosin (H&E) stain slides were prepared from formalin-fixed biopsy cores. Based on the geometry of the needle and BARD Magnum gun, we calculated the exact location of the tissue where optical characterization took place. This "spectral acquisition field" or "measurement window" is located 1.7mm from the inked-end of the core as shown in *Figure 2*. Since the area of illumination depends on probe geometry and is approximately equal to 400 µm, we have chosen a measurement window of width 0.5 mm to allow for tolerances. The FS is correlated with histopathology of tissue within this window. Tissue is classified either as benign or malignant.

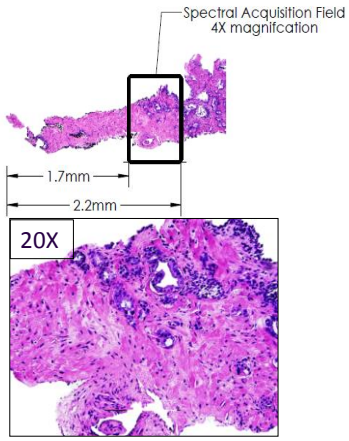

Figure 2: Location of the spectral acquisition field on a tissue biopsy core

B. *Data Analysis*

Prostate biopsies were grouped into two categories; benign and malignant. The benign category includes all biopsies that did not show any evidence of malignancy within the measurement window. FS data were processed according to the steps shown in *Figure 3*. Background was subtracted from each FS and signal-to-noise (S/N) ratio was determined. There is a degradation of the fluorescence signal when the biopsy needle is inserted into regions of the prostate with calcification, holes filled with prostatic fluids, or intersecting a previous biopsy location. These signals are unsuitable for tissue classification. Therefore, fluorescence signals with S/N $\leq$6 were excluded from the analyses. FS for 280, 290, and 300 nm excitations were trimmed at 450 nm and 330, 340, and 350 nm excitations at 540 nm. FS at each excitation was normalized to itself so that the area under the curve is unity. This eliminates inter- and intra-patient variations.

Partial least square analyses of tissue spectra was carried out to reduce data dimension and identify principal components (PC) that can be potential candidates to classify benign versus malignant tissue [11]. For all tissue samples, a set of PCs was identified using a Wilcoxon rank-sum test as showing statistically significant differences ($P < 0.05$) between benign and malignant categories. Pearson correlation coefficient was used to determine whether any of the statistically significant PCs were correlated or not. If two PCs were correlated ($R \geq 0.4$) then only one of the two PCs

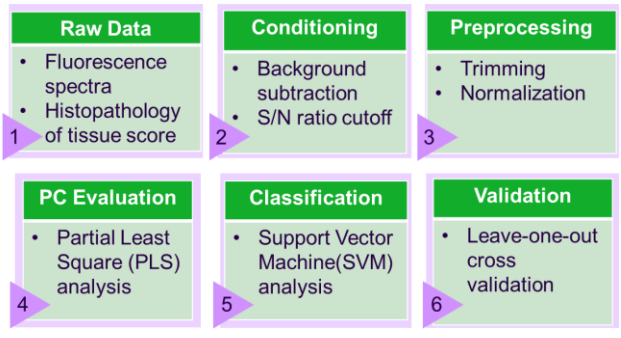

Figure 3: Steps involved in the fluorescence spectra and histopathological data analysis.

was included in the analyses. To remove data redundancy, only the PC scores that were diagnostically significant as well as least correlated with other diagnostic PCs were input into the tissue classification algorithms. Selected PCs were tested for their ability to differentiate between benign from malignant tissue using linear support vector machine (SVM) and non-linear SVM using a radial basis function (RBF) as kernel function [12]. The leave-one-out cross validation method and SVM learning were employed to determine sensitivity, specificity, negative predictive value, and positive predictive values of the tissue classification algorithm.

III. EXPERIMENTS AND RESULTS

A total 187 biopsy cores were included in the analyses. Histopathological diagnosis of tissue within the measurement window classified 109 as benign and 78 as malignant. *Figure 4A and B* show background subtracted FS for benign and malignant prostate tissue. Notable peaks include tryptophan at 340nm, collagen at 400nm, and NADH at 460nm. Normalized FS are shown in *Figure 4C*.

Table I summarizes performance of the tissue classification algorithm employing linear SVM for various combinations of PCs chosen from different excitations. The

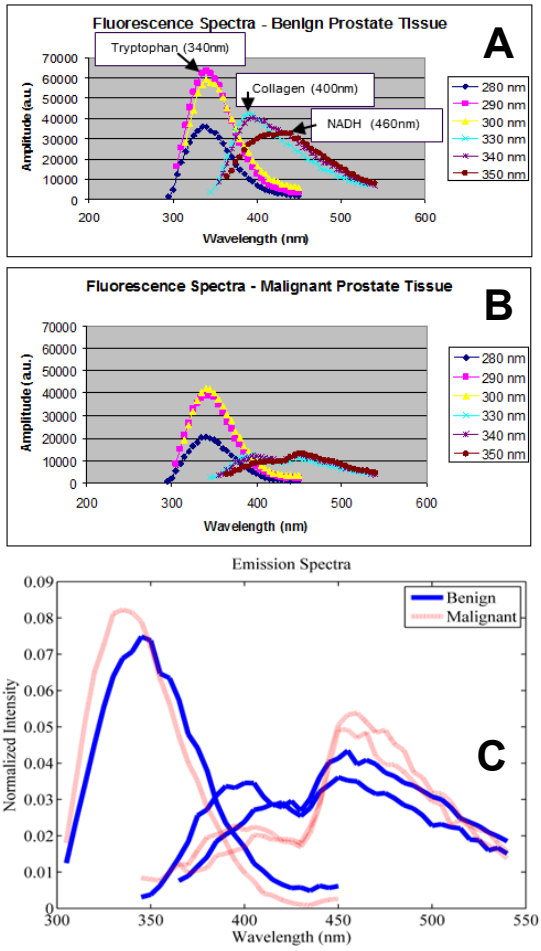

Figure 4: Fluorescence spectra of benign and malignant tissue after background subtraction (A, B) and normalized fluorescence spectra (C).

TABLE I. PERFORMANCE OF THE TISSUE CLASSIFICATION ALGORITHM

Selected Principal Components (excitation wavelengths in bold)	Sensitivity	Specificity	Negative predictive value*	Positive predictive value*
280: #1-3, 5	83%	79%	87%	74%
280: #1-3,5; **340**: #2	79%	85%	85%	79%
280: #1-3; **330**: #2,4,5	86%	83%	89%	79%
280: #1-3; **330**: #1,2,4; **340**: #1,2; **350**: #1,2	85%	85%	89%	80%
290: #1-5	80%	74%	84%	69%
290: #1-4; **340**: #3,4	82%	84%	87%	78%
290: #1-3; **330**: #1,2,4; **340**: #1,2; **350**: #1,2	86%	87%	90%	83%
300: #1,2	62%	72%	72%	61%
300: #1,2; **330**: #2,4,5	70%	82%	79%	73%
300: #1,2; **330**: #1,2,4; **340**: #1,2; **350**: #1,2	74%	82%	82%	74%

*Negative predictive values and positive predictive values were calculated without using actual disease prevalence estimates [8]

performance of the tissue classification algorithm when employing non-linear SVM with RBF as kernel function was similar to the linear SVM. The best results of 86% sensitivity and 87% specificity for malignant versus benign tissue classification were obtained when using PCs of 290, 330, 340, and 350 nm. Negative predictive value was 90%, i.e., 90% of benign tissue cores were correctly diagnosed. Positive predictive value was 83%. For only two excitation wavelengths, PCs of 280 and 330 nm returned very similar classification results. Out of three excitations tracking tryptophan, 280 and 290 nm excitations provided better classification results than 300 nm. Out of three excitations tracking collagen and NADH, 330 and 340 nm excitations were more effective than 350 nm.

IV. Conclusion

Our experimental data support potential clinical application of an optical biopsy needle based on FS for systematic prostate biopsies with increased sensitivity and specificity. Oxy- and deoxy hemoglobin interferes with the optical signals in the near UV range. Since there is no blood flow in *ex vivo* settings, it is difficult to estimate the impact of this important factor on tissue classification. For clinical applications, the configuration of the optical probe must be optimized by reducing the number of read fibers with consequent improvements in overall performance. Additional studies in human patients are required to further validate our findings.

Acknowledgment

Authors like to thank Kathy Lux for her dedication to this research project, outstanding histological work processing tissue biopsy cores and making H&E slides, and maintaining biorepository records.

References

[1] R. Siegel, J. Ma, Z. Zou, and A. Jemal, "Cancer statistics, 2014," *CA Cancer J. Clin.*, vol. 64, no. 1, pp. 9-29, Jan. 2014.

[2] H. B. Carter, P. C. Albertsen, M. J. Barry, R. Etzioni, S. J. Freedland, K. L. Greene, L. Holmberg, P. Kantoff, B. R. Konety, M. H. Murad, D. F. Penson, and A. L. Zietman, "Early Detection of Prostate Cancer: AUA Guideline," *J. Urol.*, May 2013.

[3] E. D. Crawford, D. Hirano, P. N. Werahera, M. S. Lucia, E. P. DeAntoni, F. Daneshgari, P. N. Brawn, V. O. Speights, J. S. Stewart, and G. J. Miller, "Computer modeling of prostate biopsy: tumor size and location--not clinical significance--determine cancer detection," *J Urol.*, vol. 159, no. 4, pp. 1260-1264, Apr. 1998.

[4] C. G. Drake, P. Sharma, and W. Gerritsen, "Metastatic castration-resistant prostate cancer: new therapies, novel combination strategies and implications for immunotherapy," *Oncogene*, Nov. 2013.

[5] R. Richards-Kortum and E. Sevick-Muraca, "Quantitative optical spectroscopy for tissue diagnosis," *Annu. Rev. Phys. Chem.*, vol. 47, pp. 555-606, 1996.

[6] J. Q. Brown, K. Vishwanath, G. M. Palmer, and N. Ramanujam, "Advances in quantitative UV-visible spectroscopy for clinical and pre-clinical application in cancer," *Curr. Opin. Biotechnol.*, vol. 20, no. 1, pp. 119-131, Feb. 2009.

[7] D. Evers, B. Hendriks, G. Lucassen, and T. Ruers, "Optical spectroscopy: current advances and future applications in cancer diagnostics and therapy," *Future. Oncol.*, vol. 8, no. 3, pp. 307-320, Mar. 2012.

[8] C. Zhu, E. S. Burnside, G. A. Sisney, L. R. Salkowski, J. M. Harter, B. Yu, and N. Ramanujam, "Fluorescence spectroscopy: an adjunct diagnostic tool to image-guided core needle biopsy of the breast," *IEEE Trans Biomed. Eng*, vol. 56, no. 10, pp. 2518-2528, Oct. 2009.

[9] J. L. Jayanthi, R. J. Mallia, S. T. Shiny, K. V. Baiju, A. Mathews, R. Kumar, P. Sebastian, J. Madhavan, G. N. Aparna, and N. Subhash, "Discriminant analysis of autofluorescence spectra for classification of oral lesions in vivo," *Lasers Surg. Med.*, vol. 41, no. 5, pp. 345-352, July 2009.

[10] P. N. Werahera, J. W. Daily, M. S. Lucia, A. van Bokhoven, E. D. Crawford, and F. Barnes, "Multi-Excitation Diagnostic Systems and Methods for Classification of Tissue,"US20080194969 A1, Mar. 2013.

[11] H. Martens, *Multivariate Calibration* John Wiley & Sons, New York, 1989.

[12] N. Cristianini and J. Shawe-Taylor, *An Introduction to Support Vector Machines: And Other Kernel-Based Learning Methods* Cambridge, New York: Cambridge Univ. Press, 2000.